

Investigation of oscillatory processes at peripheral plasma of vacuum spark

D.L. Kirko, O.A. Bashutin, A.S. Savjolov, P.P. Sidorov

National Research Nuclear University MEPhI, Moscow, Russia

Abstract

The properties of the plasma of a vacuum spark are studied depending on the material of the electrodes. The spectral composition of plasma radiation in the ultraviolet and visible spectral ranges has been determined. The presence of electrical oscillations in the range 1-150 MHz is recorded. The research of the microstructure of the surface of steel and copper electrodes was carried out. The presence of periodic wavelike formations with characteristic sizes in the range 2-200 μm is observed. There is a granulation of the metal surface with cell sizes in the range 0.2-1 μm .

Introduction

A low-inductance vacuum spark, along with a plasma focus, is a device for studying the processes of pinching of strong currents and the formation of dense plasma [1,2]. At the stage of pinch decay, intense plasma flows appear, which act on the surface of the electrodes. This discharge is a powerful source of electromagnetic radiation in the ultraviolet and visible ranges. In the plasma of a vacuum spark, conditions may arise for the appearance of intense high-frequency oscillations and waves [3,4]. At the same time, the presence of strong currents causes an intense effect on the surface of the electrodes in this installation. The microstructure of electrodes has been studied previously.

The experiments were carried out on the setup shown in Fig. 1. A storage capacitor with capacity 20 μF at charging voltage 5-20 kV was used to power the system. The discharge was switched on using a trigger ignition. The electrodes contained the pointed anode (1) (diameter 3-4 mm), and the cylindrical cathode (2) (diameter 15-20 mm) with the hole 1.5-2 mm in the center. In the experiments, electrodes made of steel or copper were used. The distance between the electrodes was chosen within 4-5 mm. The pressure in the chamber was in the range 10^{-4} - 10^{-5} Tor. The discharge current was in the range 100–150 kA with discharge period 6.0 μs .

Experimental setup

The action of a strong current causes intense evaporation of the anode and the central part of the cathode. Gradually, a compressed pinch (4) is formed on the discharge axis, around which the shell (5) is located (Fig. 1). When a pinch occurs near the anode, micron-sized objects are formed that emit in the x-ray range - plasma points (micropinches) (6) [2]. Photographs of the pinch region in the x-ray range of the electromagnetic spectrum ($E > 3$ keV) are shown in Fig. 2.

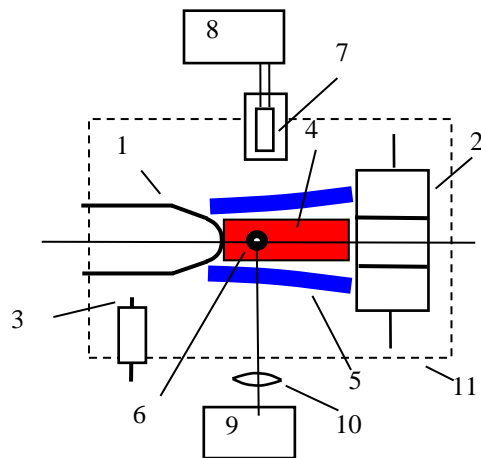


Fig. 1. Experimental setup: 1 - anode, 2 - cathode, 3 – trigger discharger, 4 – pinch, 5 – shell of discharge, 6 – plasma point, 7 – magnetic probe, 8 – analyzer of spectrum, 9 – spectrometer, 10 – objective

Images of plasma

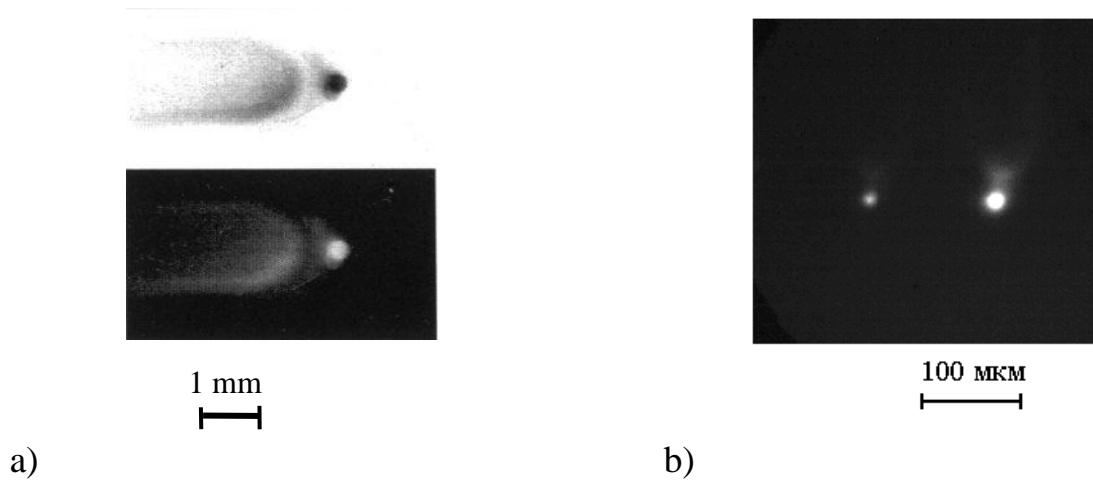
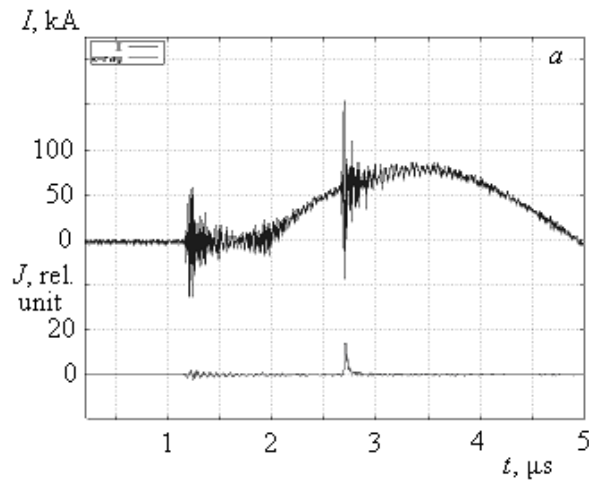


Fig. 2. Image of plasma of vacuum spark in x-ray region: a) radiation of anode and plasma point, b) plasma points

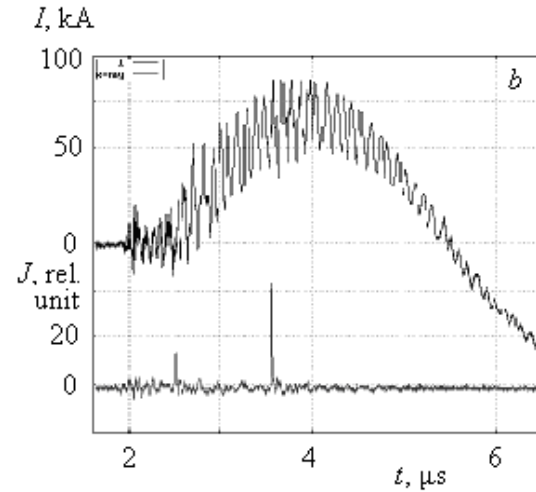
Oscillations of plasma

The study of current pulses was carried out using Rogowski coil and Tektronix TDS 2024B oscilloscope. Figure 3a shows the first half cycle of a typical current waveform with period of 6.0 μs . In the vicinity of the current maximum, the discharge is pinched and a current waist is formed, which is associated with x-ray radiation (photon energy: $E > 1 \text{ keV}$). At the moment ($t \approx 2.7 \mu\text{s}$), intense high-frequency oscillations occur in a wide range of the spectrum. These high-frequency signals were studied using low-inductance magnetic probes, which were located at different distances from the discharge. Coils (diameter 3-4 mm, number of turns 80-120) made of copper wire 0.1 mm in diameter were used for magnetic probes. When recording signals in the immediate vicinity of the pinch, the probes (7) were placed in a chamber in a protective dielectric casing (Fig. 1). The Origin computer program was used to obtain the spectrum of high-frequency oscillations. The main frequencies of these vibrations are as follows: $4.1 \pm 0.1 \text{ MHz}$, $8.3 \pm 0.2 \text{ MHz}$, $45 \pm 1 \text{ MHz}$, $92 \pm 2 \text{ MHz}$. Along with the main frequencies, the spectrum also contains a number of less intense frequencies: $18.2 \pm 0.4 \text{ MHz}$, $35 \pm 1 \text{ MHz}$, $67 \pm 1 \text{ MHz}$, $81 \pm 2 \text{ MHz}$. The spectrum of high-frequency oscillations of the discharge current is shown in Fig. 4.

Current of the discharge



a)



b)

Fig. 3. Oscillograms of the discharge current and impulse of x-ray radiation: a) characteristic view of impulses, b) intensive high frequency oscillations

Spectrum of oscillations

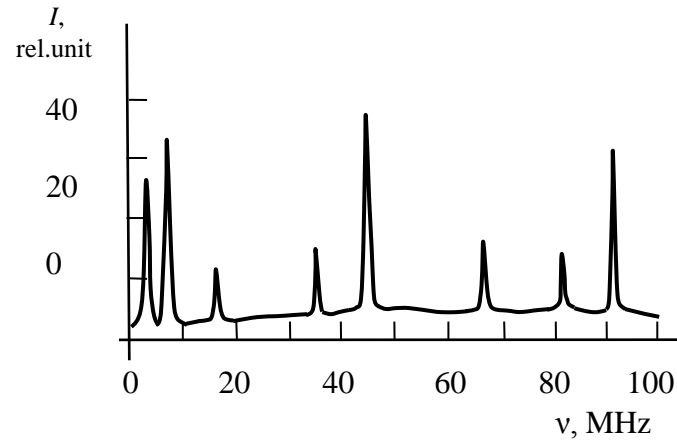


Fig. 4. Spectrum of high frequency oscillations of the discharge current

Let us estimate the characteristic frequencies of processes for a plasma in a vacuum spark. With the plasma parameters in the pinch: concentration $n_e=1.2 \cdot 10^{19} \text{ cm}^{-3}$, temperature $T=2.5 \cdot 10^5 \text{ K}$, the plasma frequencies are: $\omega_{pe} = (4\pi n_e e^2 / m_e)^{1/2} = 1.9 \cdot 10^{14} \text{ s}^{-1}$ $\omega_{pi} = (4\pi n_e e^2 / m_p)^{1/2} = 4.5 \cdot 10^{12} \text{ s}^{-1}$

These frequency values are much higher than the frequencies recorded in the experiments. At characteristic currents flowing through the pinch plasma $I = 100\text{-}110 \text{ kA}$, for the magnetic field $B = 3 \cdot 10^4 \text{ Gs}$, the ion cyclotron frequency takes on the value $\omega_{Bi} = eB / m_p = 2 \cdot 10^8 \text{ s}^{-1}$, and the electron cyclotron frequency, respectively: $\omega_{Be} = eB / m_e = 3.6 \cdot 10^{11} \text{ s}^{-1}$. Therefore, the experimentally observed oscillation frequencies $\nu = 1\text{-}110 \text{ MHz}$ will be located in the range of low-frequency branches of plasma waves. For the propagation of plasma waves along the magnetic field for electron-cyclotron and ion-cyclotron waves, the dispersion equation has the form [5]: $k^2 = \omega^2 / c^2 [1 - (\omega_{pe}^2 + \omega_{pi}^2) / ((\omega - \omega_{Be})(\omega + \omega_{Bi}))]$

When using this expression at a frequency $\nu=92 \text{ MHz}$, the wavelength and velocity of the electron cyclotron wave will be as follows: $\lambda=3.1 \cdot 10^{-2} \text{ cm}$ and $v=2.4 \cdot 10^6 \text{ cm/s}$.

Spectral measurements

Ava Spec 2048 spectrometer (spectral range 200-1100 nm, resolution 0.3 nm), MUM monochromator (spectral range 200-800 nm, resolution 1.5 nm), and FEU-85 photomultiplier were used to study the radiation from the peripheral plasma. The equipment was calibrated using a SIRSh8-200 lamp. Radiation was recorded from a plasma envelope 9-12 mm in diameter. For the experiments, we used a cathode and anode made of steel. The most intense lines of elements (Fig. 5) included in the composition of the electrodes are the lines of iron atoms: Fe I 298 nm, 382 nm; iron ions: Fe II 270 nm, 361 nm, 523 nm; silicon ions: Si II 305 nm; carbon atoms C I 601 nm. The atomic lines of nitrogen: N I 415 nm, 493 nm, and oxygen and nitrogen ions: O II 253 nm, N II 464 nm are the lines of elements arising from the ionization of the residual gas. At the same time, the hydrogen lines H_α 656 nm and H_γ 434 nm are recorded. The time course of these lines was obtained using the monochromator. The H_α line is more intense. There is also a strong continuous spectrum in the radiation. The time dependences of the line intensities exhibit oscillatory processes at frequencies 3.2 ± 0.1 MHz and 10.5 ± 0.2 MHz, which are close to those obtained from current measurements.

It was assumed that the model of local thermal equilibrium is realized for the shell plasma [6]. Therefore, it is possible to use the method of relative intensities of spectral lines. The hydrogen lines H_α and H_γ were used to calculate the values of the plasma temperature for various discharge modes. For a discharge at charging voltage $U_c=16$ kV, the temperature value $T=8200 \pm 300$ K was obtained. This temperature value is more than an order of magnitude lower than the values existing in the pinch region.

The spectral lines of atomic hydrogen H_γ и H_α (Fig. 5) exhibit significant broadening in the range 2.0-10.0 nm. The contours of these lines are dispersive. Assuming the existence of micro fields in the plasma, the plasma concentration was calculated from the Stark broadening of these lines, which was $n_e=(3.4 \pm 0.3) \cdot 10^{16} \text{ cm}^{-3}$ (charging voltage $U_c = 16$ kV). This concentration value is approximately two orders of magnitude less than that present in the pinch region.

Spectrum of plasma

The continuous spectrum component was recorded in the entire recording range of the spectrometer (200-1100 nm). This dependence is superimposed on fairly intense lines in the ultraviolet range (240-310 nm) and (350-400 nm), in the visible range (400-470 nm) and (480-540 nm). The continuous spectrum has a noticeable decrease in the range 320-360 nm. In view of the complexity of this dependence, it is possible only approximately to approximate the continuous spectrum by the Planck distribution with temperature $T \approx 9400$ K.

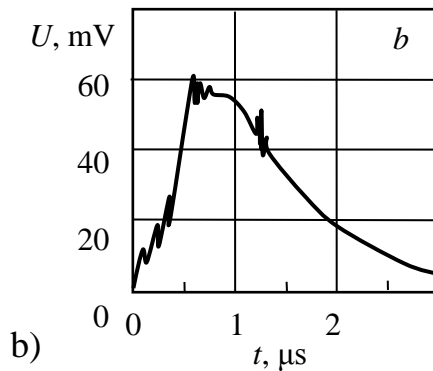
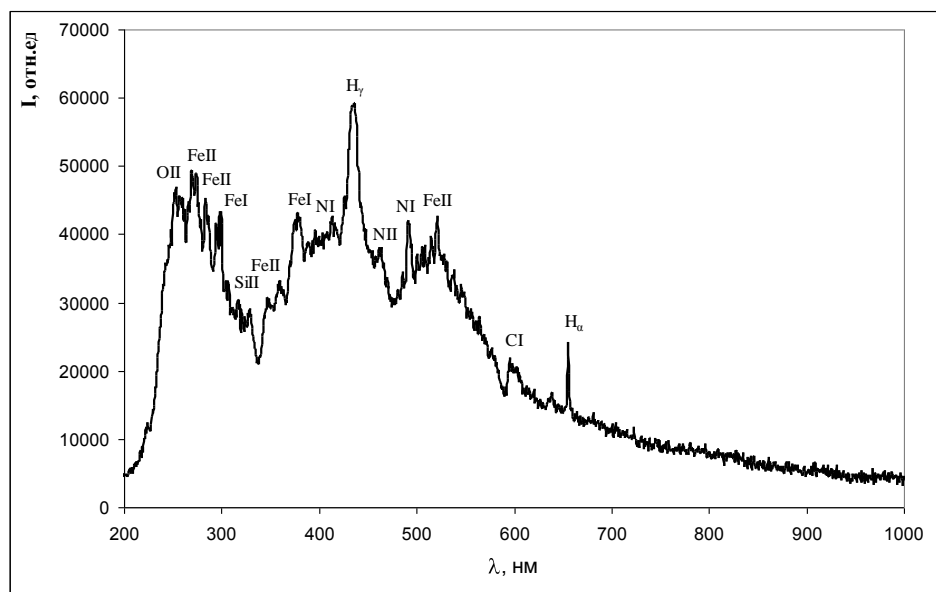
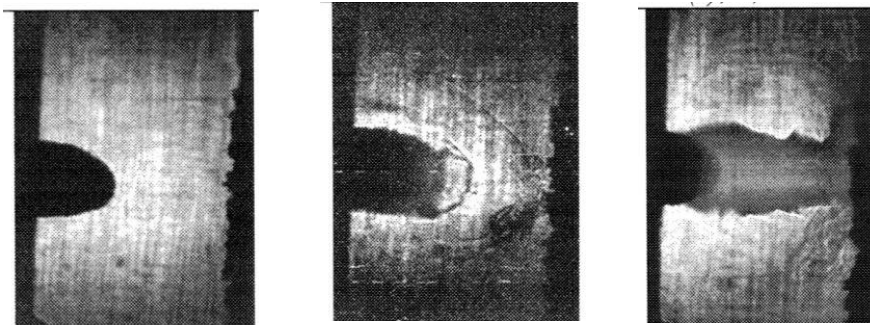


Fig. 5. Spectral measurements of the vacuum spark: a) spectrum of discharge radiation, b) temporal dependence of radiation of hydrogen line H γ 434 nm

Laser measurements

In Fig. 6 shows shadowgrams of the pinch plasma obtained with a nitrogen laser. For the process of pinch formation, the appearance of a plasma waist is typical, as a rule, in the time interval $t=1.1-1.2 \mu\text{s}$ from the beginning of the discharge. In laser measurements performed with the nitrogen laser ($\lambda=337 \text{ nm}$, $\Delta t=3 \text{ ns}$) and a Mach-Zehnder interferometer, the radial distributions of the electron concentration were obtained at various distances from the anode. Based on these results, it can be concluded that the pinch plasma has a shape close to cylindrical (diameter 0.8-1.0 mm). In this case, the concentration value on the surface of the cylinder is approximately 4 times the value on the axis. The maximum plasma concentration was $n_e \approx 5 \cdot 10^{17} \text{ cm}^{-3}$.



$t=0.5 \mu\text{s}$

$t=1.1 \mu\text{s}$

$t=1.5 \mu\text{s}$

Fig. 6. The shadowgram of discharge of the vacuum spark

Research of surface of electrodes

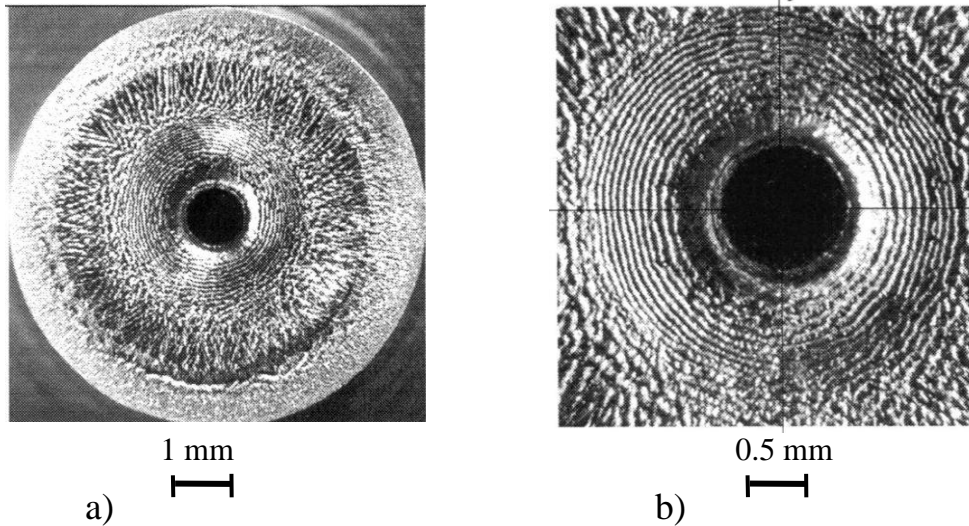


Fig. 7. Ring structures on the cathode surface: a) view of cathode, b) region near the hole

According to studies of these discharges, the main current in the range 100–150 kA flows through the pinch region [1,2]. A smaller part of the current flows through the peripheral plasma layer. The greatest impact from the currents is experienced by the sharpened surface of the anode and the surface of the cathode near the central hole. Earlier, concentric rings were found on the cathode surface near the central hole (Fig. 7) and their parameters were recorded [2,4]. The distance between two adjacent rings is in the range 150-250 μm . The height of the rings is in the range 10-60 μm . In turn, these rings on the cathode can consist of individual tubercles, hills with sizes 100-150 μm . The formation of this ring structure is apparently associated with the action of plasma waves on the material surface.

Surface of electrodes

Let us consider the result of plasma interaction with the anode surface (Fig. 1). This electrode is usually made of steel and has diameter 3-4 mm, the radius of curvature of the tip is 1-1.5 mm. In the first half-period of the current, a positive potential is applied to this electrode and, according to the data of electrical and x-ray measurements, the surface is exposed to a powerful flow of electrons with energy density 30-50 J/mm². The microstructure of the electrode surface was investigated using Hitachi TM1000 and VEGA 3 SEM electron microscopes. On the surface of the anode, after exposure to plasma, the appearance of a wavy relief is observed (Fig. 8 abc). These structures, up to 5-7, similar to waves with a wavelength of about 220-250 μm , are directed to the rounded end of the anode. Smaller waves with wavelengths of about 10-20 μm are located on almost every crest of these waves. The smallest waves with wavelengths of about 2-3 microns are observed at these waves. At the same time, the surface also contains formations similar to flakes or fluff with sizes 10-40 μm (Fig. 8d). On areas of the surface near height 20-40 μm , areas are formed containing metal granulation with a cell size in the region 0.2-1 μm (Fig. 8f).

Images of surface of electrodes

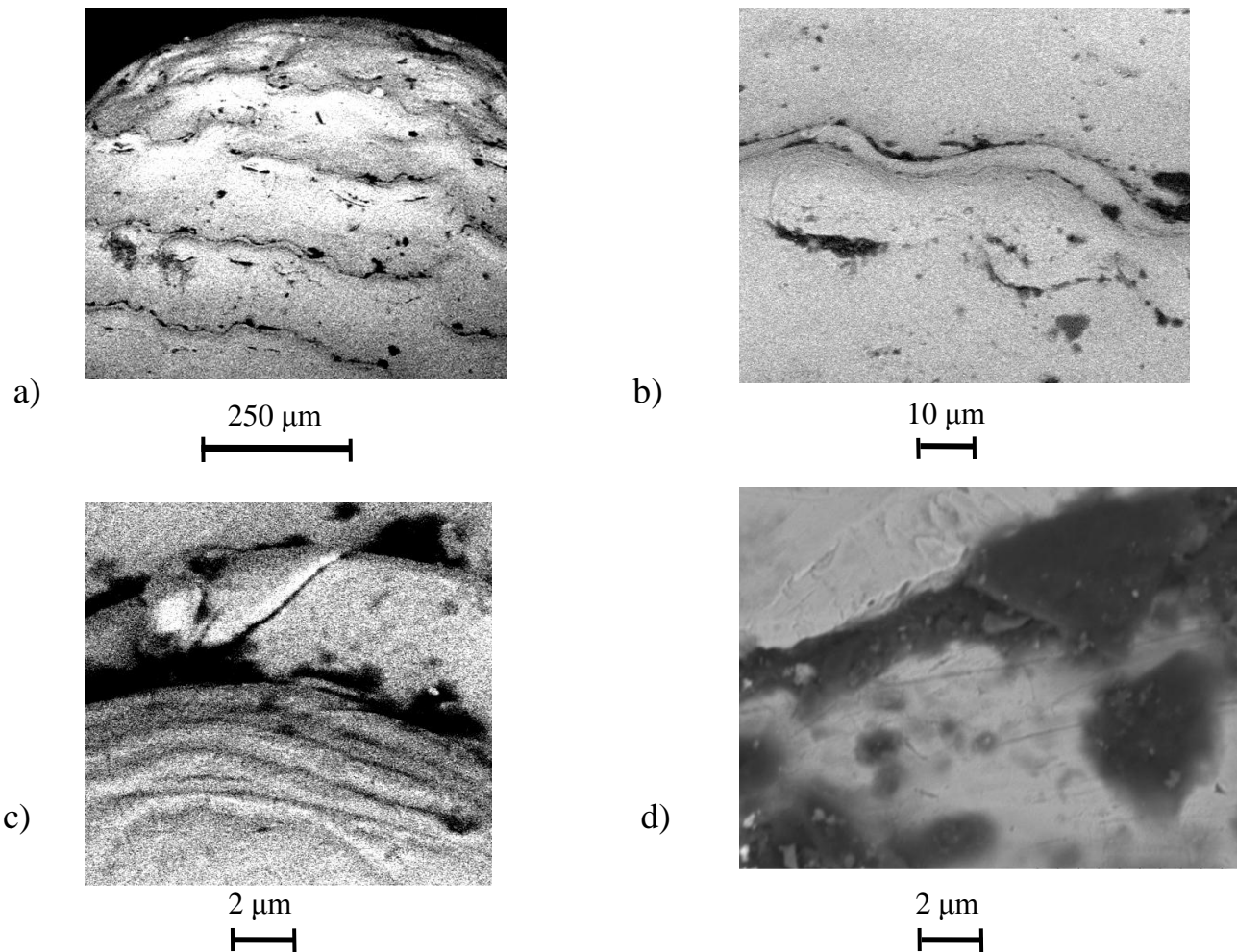


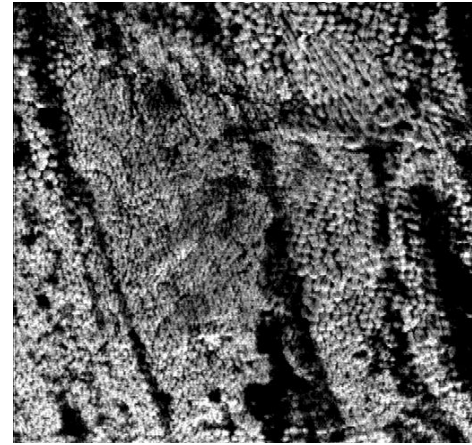
Fig. 8. Images of the surface of steel anode: a) wave relief on the surface, b) image of separate wave, c) smallest waves, d) "fluff", "flakes", e) "hills", "bumps", f) cellular structure of anode surface

Surface. Images



e)

10 μm
┌───┐



f)

2 μm
┌───┐

Fig.8. Images of surface of steel anode: e) “hilld”, “bumps”, f) cellular structure of anode surface

Surface of electrodes

Strong currents flowing through the discharge plasma act on the anode surface. This leads to heating and melting of the surface layer of the metal during the first half-period of the current $t \approx 3 \mu\text{s}$. The relief of the anode surface can show the characteristic dimensions of the current inhomogeneities, or its division into smaller currents with dimensions 10-50 μm . The total current duration is usually 3-4 half cycles or 9-12 μs . After melting the surface layer 50-100 μm thick, the cessation of the current can cause rapid crystallization of the metal. In this case, the formation of granulation is observed for many alloys containing iron [7].

Consider the process of formation of undulating structures on the surface of a pointed steel anode. It was suggested that the 50-100 μm thick surface layer of the anode under the influence of intense electron beams melts. Let us assume that the time during which the liquid state of the surface layer is maintained is about 10-15 μs . Earlier, for the peripheral plasma of a vacuum spark, plasma ion-cyclotron electron and ion waves with wavelengths 0.1–5 mm at frequencies 100 kHz – 100 MHz were considered [4]. This will mean the possibility of these waves acting on the surface of the molten electrode. Such phenomena can be simulated in laboratory conditions and at large times of the order 10-100 ms [7]. During these experiments, traces of impact, including wavy ones, can remain on the surface of the molten metal. Therefore, it can be assumed that at the stage of cooling and crystallization of the molten surface layer of the electrode, this wave structure of the plasma wave can retain its image.

Structures on the river sand

Structures “riffles”



a)



b)

Fig. 9. Structures on the river sand: “riffles”. The coast of the Volga river near city Kazan.

Structures on the surface

Consider the observed structure and lengths of the observed wavelike images on the surface. An interesting fact of these surfaces is the existence of “long” waves with wavelength about 100–150 μm (Fig. 8a), on which “medium” waves appear, with wavelengths of about 10–20 μm (Fig. 8b). In turn, the “middle” ones can appear shorter, wavelengths 0.5–2 μm . The sizes of the considered waves differ approximately 10 times. Repetition, reproducibility of the structure when changing the scale for physical objects is usually associated with the concept of fractality.

A similar effect occurs in nature for sea and river waves on the surface of the sandy bottom, which is usually called the formation of “riffles” [8, 9]. You can see these wave structures on the river sand, the river Volga placed on the right, the coast of city Kazan – on the left (Fig. 9). The complete structure of these sand formations contains higher ridges, having wavelengths comparable to those of normal coastal sea or river waves, for example, with wavelength 1-2 m. And smaller undulating formations on “ripple” sands, with wavelengths, for example 5 -20 cm. These small waves can exist on the water surface only in the form of small, unstable ripples. Therefore, in view of the pattern on the sandy bottom, there must be a mechanism leading to the formation of these small waves. Here an analogy arises with an increase in frequency or a decrease in wavelength inherent in nonlinear wave effects [9, 10].

A simpler variant is the case of electron waves in plasma, described using the Klein-Gordon equation [5]. Along with the fundamental frequency, the appearance of multiple frequencies, harmonics, expressed by the formula: $\omega_k = \omega \cdot 2^k$, is also possible.

As a curious phenomenon on the surface of the steel anode, the appearance of formations similar to a kind of “fluff” should be noted (Fig. 8d). Similar phenomena were found on tungsten surfaces in devices associated with high-temperature plasma of the tokamak type. At the same time, a micron cellular structure appears in some areas of the steel anode surface (Fig. 5b) [4]. Similar phenomena are observed during rapid crystallization of the melt [7].

Conclusion

The parameters of the peripheral plasma of the vacuum spark are investigated. High-frequency oscillations in the plasma are fixed and the spectrum of these oscillations is constructed in the 1-110 MHz range. A number of characteristic intense frequencies stand out in the spectrum. The analysis of the possibility of the existence of various waves in the plasma shell of the vacuum spark is carried out. The registered high-frequency oscillations are related to the appearance of electron-cyclotron and ion-cyclotron waves in the vacuum spark plasma. The study of the properties of the peripheral plasma of the vacuum spark has been carried out. Spectral studies made it possible to determine the plasma temperature $T=8200\pm 300$ K and the plasma concentration $n_e=(3.4\pm 0.3)\cdot 10^{16}$ cm⁻³ of the plasma envelope. The microstructure of the electrodes of the vacuum spark installation is investigated. A characteristic wavy relief is observed on the surface of the steel anode, due to the effect of strong currents.

References

1. A.G. Rousskikh, R.B. Baksht, A.S. Zhigalin, V.I. Oreshkin, S.A. Chaikovsky, N.A. Labetskaya, "Multichannel vacuum arc discharge for z-pinch formation," *Plasma Physics Reports*, vol. 38, Is. 8, pp. 595-607, August 2012.
2. O.A. Bashutin, A.S. Savjolov, "Suprathermal electrons in a vacuum spark discharge," *Plasma Physics Reports*, vol. 42, Is. 4, pp. 347-354, April 2016.
3. D.L. Kirko, A.S. Savjolov, S.A. Sarancev. *Vestnik Kazan technologic university*. 2011, V.14, N.15, pp.82-85.
4. D.L. Kirko, A.S. Savelov, "Wave processes in the plasma of a low-inductive vacuum spark," *Russian Physics Journal*, vol. 57, No. 11, March 2015.
5. N.A. Kroll, A.W. Trivelpiece, "Principles of plasma physics," New York: McGrawHill, 1973.
6. R. Huddlstone, S. Leonard, "Plasma diagnostic techniques," New York: Academic Press, 1965.
7. A.M. Glezer, I.E. Permjakova, "Nanocrystals tempered from melting," Moscow: Fizmatlit, 2012.
8. B.B. Kadomtsev, "Common phenomena in plasma," Moscow: Nauka, 1988.
9. B.B. Kadomtsev, V.I. Rydник, "Waves around us", Moscow, Knowledge, 1981.
10. B.B. Kadomtsev, V.I. Karpman, "Nonlinear waves", 1971, UFN, V.103, N.2, pp.193-232.